Radiation Pattern Diversified Double-Fluid-Channel Surface-Wave Antenna for Mobile Communications

Yuanjun Shen
Dept. of Electronic and Electrical Eng.
University College London
London, UK
yuanjun.shen@ucl.ac.uk

Kin-Fai Tong
Dept. of Electronic and Electrical Eng.
University College London
London, UK
k.tong@ucl.ac.uk

Kai-Kit Wong
Dept. of Electronic and Electrical Eng.
University College London
London, UK
kai-kit.wong@ucl.ac.uk

***Abstract*—In this paper, we present an antenna design for millimeter wave 5G applications. The proposed antenna has a wide working frequency range from 23.5 GHz to 36.5 GHz. This can cover the millimeter wave 5G frequency band in most countries. The design is simple and will mitigate the difficulty when implementing in a wireless system with reconfigurable capability. The antenna design only needs a single RF port as input to achieve radiation pattern diversity by moving the fluid radiators in its two channels. With the radiation pattern diversity capability, the problem like weak signal strength and inter channel interference can be eased.**

The design shows higher dynamic range of patterns turning when compare to the previous work on single-channel surface-wave antenna with the purpose of wider angular coverage with multichannel design. The comparison result of the two designs will also be provided in this paper.

***Index Terms*—Reconfigurable Antenna, Fluid Antenna, Liquid Metal, Galinstan, MIMO, Surface Wave, Radiation Pattern Diversity**

I. Introduction

Antenna arrays play a critical role in modern wireless world, particularly in mobile communications [1]. Now with the 5G rollout, antenna arrays become essential to communication system [2] due to the quasi optic nature of 5G frequencies [3]. Alongside the improvement of chip and advanced DSP algorithm, the beam-forming feature is reliable and smooth. However, this feature can hardy be found on portable devices. Firstly, antenna arrays need much more space than single antenna [2]. Secondly, multiple antennas need multiple RF front ends, which will not only take more spaces but also increase the complexity and raise the cost [4]. Even some high-end smartphone equipped with an antenna array [2], the overall performance improvement is limited as the design will be restricted within the physical shape of the smartphones substantially. The proposed antenna was designed to tackle such perplexity. To achieve the capability such as radiation pattern diversity without antenna array technique, a double-channel surface wave fluid antenna has been introduced.

Fluid antennas can obtain reconfigurability by moving the fluid radiators inside the antenna structures in a controlled manner [5], [6]. So that the antenna performance, such as operating frequency, polarization, can be adjusted. Fluid antennas can also reduce the size of antenna system when compared to antenna arrays. However, the multiple signal feeding ports issue still exist. For instance [7], the fluid radiator can travel along the fluid channel and when fluid radiator locates at different positions, a different feeding port is needed to excite the antenna. Therefore, the system will require multiple RF chains just like the antenna arrays [8].

The proposed design brings in surface-wave technique to deal with the issue [9], [10]. By adding a surface wave launcher, the surface wave excited can propagate along the entire fluid channel. Therefore, no matter where the fluid radiator stops inside the channel, it can always be fed [11]. In this way, the multi RF front ends are not necessary, and the system can be significantly simplified. Moreover, the PCB surface wave launcher can be integrated with other RF modules to further improve the performance of the wireless system.

Double-fluid-channel design is proposed in contrast to the single channel case [12] investigating the potential improvement over radiation pattern diversity. As the proposed one has more flexibility on two separated channels.

II. ANTENNA GEOMETRY

Fig. 1 shows the transparent perspective view of the proposed double-channelled fluid antenna. The proposed antenna structure mainly has five parts: (i) a PCB substrate on the bottom, (ii) a surface wave launcher engraved on the top of the PCB by laser cutting, (iii) a fluid container with built-in fluid channels, (iv) two liquid metal radiators and (v) a 2.92 mm RF connector.

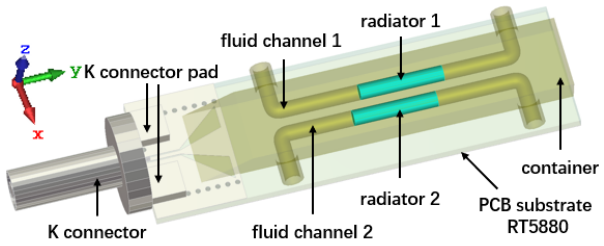

Fig. 1. The perspective view of the proposed antenna design.

The 2.92 mm RF connector is a simplified model of a real RF connector which will be connected to the fabricated antenna. The PCB substrate is made of Rogers RT5880 laminates

($\varepsilon_r = 2.2$, thickness = 0.787 mm and $tan(\delta) = 0.0009$ at 10 GHz). The substrate has a ground plane on the bottom and a surface wave launcher on the top, both copper cladding layers have a thickness of 35 μm. The fluid container sitting on the top of the PCB substrate is 3D printed, and the material is epoxy resin ($\varepsilon_r = 4.0$). The fluid radiators inside the channels of the fluid container are liquid metal Galinstan (electric conductivity $= 3.46 \times 10^6 S/m$, thermal conductivity = 16.5 W/K/m, material density $= 6440 kg/m^3$, thermal diffusivity $= 8.65578 \times 10^{-6} m^2/s$).

(a) Side View

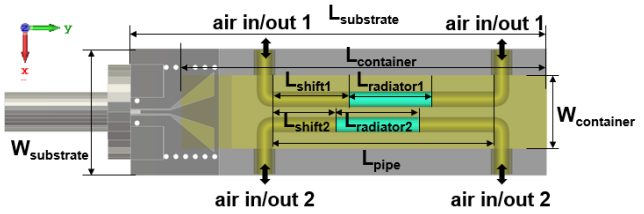

(b) Top View

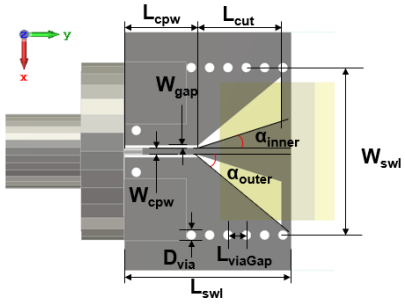

(c) surface wave launcher pattern

Fig. 2. The (a)side view, (b)top view, and (c)the pattern of the surface wave launcher of the proposed antenna.

Fig. 2a and 2b provide the side and top view of the antenna structure. Fig. 2c depicts the details of the surface wave launcher pattern. All figures are marked with parameters, which values are listed in Table I. The antenna structure has an overall dimension (without the K connector) of ($L_{substrate} \times W_{substrate} \times (H_{container} + H_{subsrate})$), $33 \times 10 \times 2.8\, mm^3$.

III. OPERATING PRINCIPLE

When signal is fed in by the 2.92 mm connector, and the signal reach surface wave launcher structure through the transmission line, the surface wave launcher performs as a converter which transforms the signal into surface wave. Afterwards, the surface wave travels forward along the positive y-direction on the top side of the dielectric substrate. As shown in Fig. 2b, the fluid radiators inside the fluid channel can now be excited and scatter electromagnetic wave out to free space. The inlets/outlets are connected to a pump system so that the position of both fluid radiators can be precisely controlled independently. The E-field distribution on the antenna in Fig. 3 verifies the explanations. Moreover, in the comparison of the case without the fluid radiators shown in Fig. 3a, Fig. 3b and Fig. 3c demonstrates that the fluid radiators alter the scattering of the surface wave. And different combinations of fluid radiator positions can shape the E-field into different distribution.

TABLE I
ANTENNA PARAMETERS

$L_{substrate}$	33.0 mm	$W_{substrate}$	10.0 mm
$L_{container}$	29.0 mm	$W_{container}$	5.8 mm
$H_{substrate}$	0.787 mm	$H_{container}$	2.0 mm
$D_{channel}$	1.2 mm	$L_{channel}$	17.5 mm
$L_{radiator1}$	6.5 mm	L_{shift1}	6.0 mm
$L_{radiator2}$	6.5 mm	L_{shift2}	5.0 mm
D_{via}	0.4 mm	W_{viGap}	0.8 mm
L_{cpw}	3.1 mm	W_{cpw}	0.3 mm
L_{swl}	7.0 mm	W_{swl}	7.0 mm
L_{cut}	3.5 mm	W_{gap}	0.1 mm
α_{inner}	20°	α_{outer}	42°
$\alpha_{container}$	26°	H_{copper}	0.035 mm

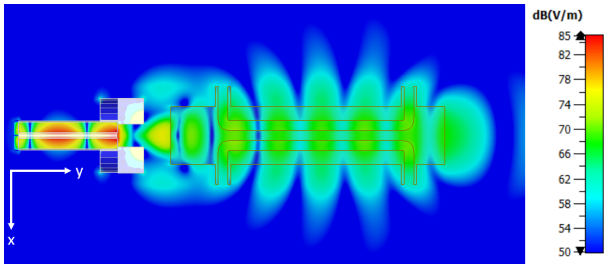

(a) without fluid radiator

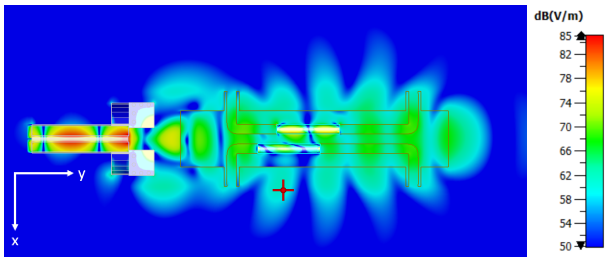

(b) with fluid radiator in case 1

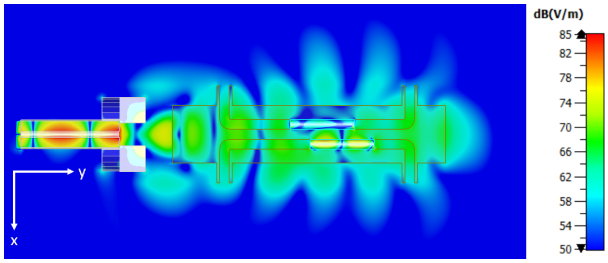

(c) with fluid radiator in case 2

Fig. 3. The comparison of the E-field distribution of the antenna (a)without fluid radiators, (b)with fluid radiators at case 1($L_{shift1} = 4mm, L_{shift2} = 2mm$), (c)with fluid radiators at case 2 ($L_{shift1} = 6mm, L_{shift2} = 8mm$ from top view at 26 GHz, cut at z = 1.5 mm.

Therefore, the radiation pattern changes accordingly. This scattering effect is demonstrated in Fig. 3 and Fig. 4. The results of two different position combinations (case1 and case2) of the fluid radiators demonstrate an obvious affection on *E*-field distribution. Consequently, radiation pattern diversity can be achieved by relocating the fluid radiators.

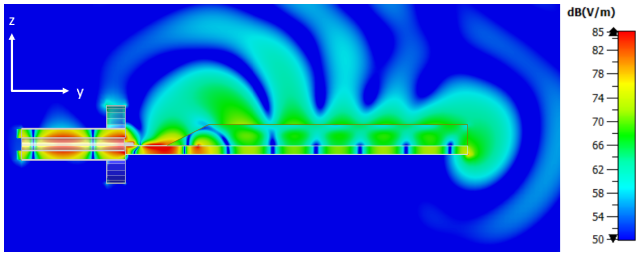

(a) without fluid radiator

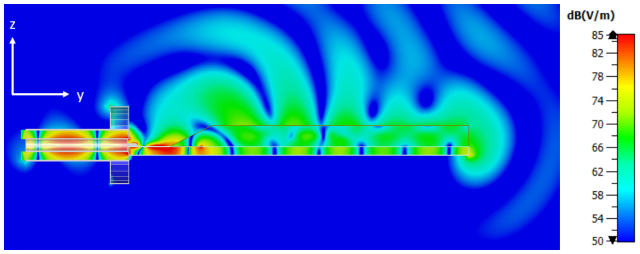

(b) with fluid radiator in case 1

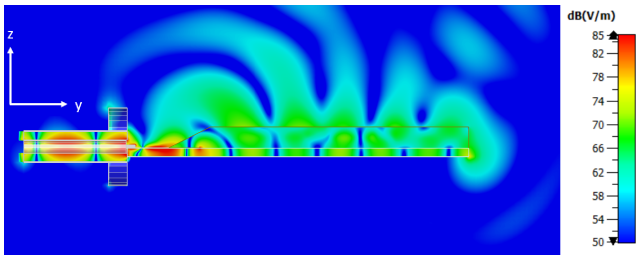

(c) with fluid radiator in case 2

Fig. 4. The comparison of the *E*-field distribution of the antenna (a)without fluid radiators, (b)with fluid radiators at case 1($L_{shift1} = 4mm, L_{shift2} = 2mm$), (c)with fluid radiators at case 2 ($L_{shift1} = 6mm, L_{shift2} = 8mm$) from side view at 26 GHz, cut at x = 0 mm.

IV. SIMULATED RESULTS

One of the main features of the proposed antenna is its multi-fluid channels when compared to the single channel design [12]. The double-channel design can facilitate more different combinations of radiators. Therefore, the number of different radiation patterns can be increased. Moreover, as the fluid radiators can be shifted to different position independently, the radiation pattern in the *x*-direction can be changed as well.

In the simulation, each radiator has 6 different positions from L_{shift1} *and* $L_{shift2} = 0mm$ *to* $10mm$ in a 2 mm step along the fluid channel. Therefore, the design has 36 different fluid radiator combinations in total. The S_{11} results of the antenna model is shown in Fig. 5. The results show the antenna has an operating frequency ranged from 23.5 to 36.5 GHz ($|S_{11}| < -10dB$) for all 36 fluid radiator positions. For clarity, only the results of case1 ($L_{shift1} = 4mm, L_{shift2} = 2mm$) and case2 ($L_{shift1} = 6mm, L_{shift2} = 8mm$) are highlighted and the S_{11} of the case without the fluid radiator is also provided as reference.

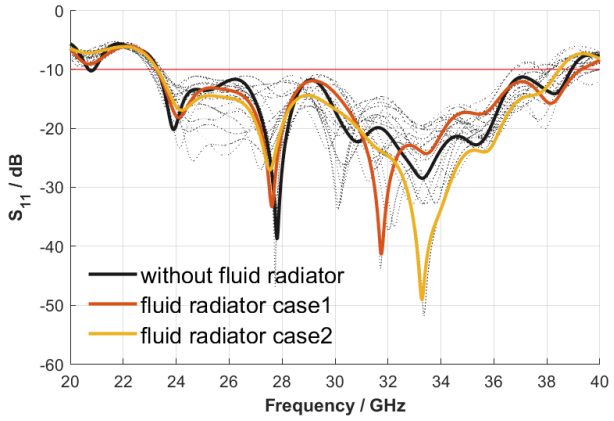

Fig. 5. S_{11} results of the antenna of the 36 radiator positions with highlighted curves indicating case 1($L_{shift1} = 4mm, L_{shift2} = 2mm$), case 2($L_{shift1} = 6mm, L_{shift2} = 8mm$) and the case of no fluid radiator for reference.

The radiation pattern diversity capability of the antenna can be explained with the analysis of the simulation result shown in Fig. 6. The figure combines all the 36 far field radiation patterns of the antenna at 26 GHz. All these results are shown by dotted lines. The two highlight lines demonstrate the maximum and minimum bounds of the results. The gap between the maximum and the minimum bounds is the dynamic range of realized gain the antenna could achieve by shifting the position of fluid radiators.

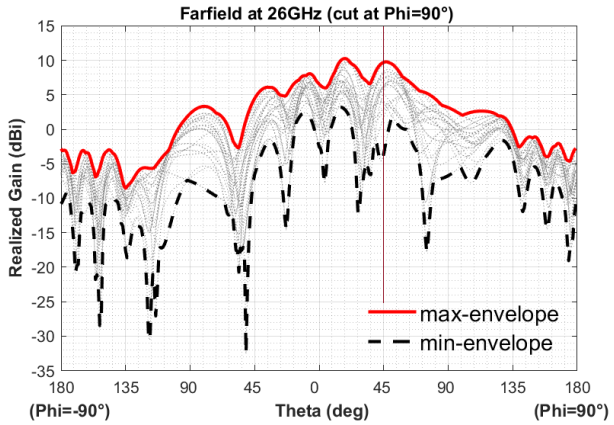

Fig. 6. The maximum and minimum envelop of the far field radiation pattern of the antenna at 26 GHz.

For example, the maximum and minimum realized gains the antenna could obtain at the angle $(\theta, \phi) = (45°, 90°)$, as reference line shown, are around 10 dBi and -5 dBi respectively. This 15 dB gap is the dynamic range that can be achieved by moving the fluid radiators. The proposed antenna has a maximum dynamic range of 33.93 dB at (50º,-90º), and has an average dynamic range of 10.02 dB across the whole

360º. The comparison result of dynamic range of the single and double channel antenna design is shown in Table II. It can be observed that the proposed double-channel antenna has a 0.95 dB increase on average dynamic range and 8.46 dB increase on maximum dynamic range.

TABLE II
COMPARISON OF THE SINGLE AND DOUBLE CHANNEL DESIGN

Design	Single Channel	Double Channel
Avg. Dynamic Range	9.07 dB	10.02 dB
max. Dynamic Range	25.47 dB	33.96 dB
max. DR angle	(34º,90º)	(50º,-90º)

When a user at a specific direction needs a signal strength improvement, the antenna could shift the fluid radiators to make the antenna get the maximum gain at the required direction. Moreover, the antenna could also actively eliminate the interference signal by shifting a null to the interference direction.

V. CONCLUSION

The proposed fluid antenna has a small physical size and simple design compared with conventional fluid antenna designs. It has a wide working frequency range which covers the very high 5G Frequency bands [13]. And it could deliver radiation pattern diversity by shifting its fluid radiators which gives a more flexible antenna configuration. The maximum and average dynamic range of the design is 8.46 dB and 0.95 dB respectively higher than the single channel case.

ACKNOWLEDGMENT

This work was supported in part by the Engineering and Physical Science Research Council (EPSRC) under grant EP/V052942/1.

REFERENCES

[1] S. Yang and L. Hanzo, "Fifty years of mimo detection: The road to large-scale mimos," *IEEE Communications Surveys Tutorials*, vol. 17, no. 4, pp. 1941–1988, 2015.

[2] K.-L. Wong, C.-Y. Tsai, J.-Y. Lu, D.-M. Chian, and W.-Y. Li, "Compact eight mimo antennas for 5g smartphones and their mimo capacity verification," in *2016 URSI Asia-Pacific Radio Science Conference (URSI AP-RASC)*, pp. 1054–1056, 2016.

[3] P. A S, G. A. Bidkar, T. D, Nagaraj, S. M P M, and Vishal, "Design of compact beam-steering antenna with a novel metasubstrate structure," *2020 IEEE International Conference on Distributed Computing, VLSI, Electrical Circuits and Robotics (DISCOVER)*, pp. 96–99, 2020.

[4] N. Ojaroudiparchin, M. Shen, and G. F. Pedersen, "Multi-layer 5G mobile phone antenna for multi-user MIMO communications," *2015 23rd Telecommunications Forum, TELFOR 2015*, pp. 559–562, 2016.

[5] Y. Shen, K. F. Tong, and K. K. Wong, "Beam-steering Surface Wave Fluid Antennas for MIMO Applications," in *Asia-Pacific Microwave Conference Proceedings, APMC*, vol. 2020-Decem, pp. 634–636, 2020.

[6] C. Borda-Fortuny, L. Cai, K. F. Tong, and K. K. Wong, "Low-Cost 3D-Printed Coupling-Fed Frequency Agile Fluidic Monopole Antenna System," *IEEE Access*, vol. 7, pp. 95058–95064, 2019.

[7] K. K. Wong, A. Shojaeifard, K. F. Tong, and Y. Zhang, "Fluid Antenna Systems," *IEEE Transactions on Wireless Communications*, vol. 20, no. 3, pp. 1950–1962, 2021.

[8] K. K. Wong, A. Shojaeifard, K. F. Tong, and Y. Zhang, "Performance Limits of Fluid Antenna Systems," *IEEE Communications Letters*, vol. 24, no. 11, pp. 2469–2472, 2020.

[9] S. K. Podilchak, A. P. Freundorfer, and Y. M. Antar, "Planar surface-wave sources and metallic grating lenses for controlled guided-wave propagation," *IEEE Antennas and Wireless Propagation Letters*, vol. 8, pp. 371–374, 2009.

[10] Y. Shen, K. F. Tong, and K. K. Wong, "Reconfigurable Surface Wave Fluid Antenna for Spatial MIMO Applications," in *2021 IEEE-APS Topical Conference on Antennas and Propagation in Wireless Communications, APWC 2021*, pp. 150–152, 2021.

[11] J. L. Liu, T. Su, and Z. X. Liu, "High-Gain Grating Antenna with Surface Wave Launcher Array," *IEEE Antennas and Wireless Propagation Letters*, vol. 17, no. 4, pp. 706–709, 2018.

[12] Y. Shen, K. F. Tong, and K. K. Wong, "Radiation Pattern Diversified Single-Fluid-Channel Surface-Wave Antenna for Mobile Communications," *manuscript submitted for publication*, 2022.

[13] W. Hong, Z. H. Jiang, C. Yu, D. Hou, H. Wang, C. Guo, Y. Hu, L. Kuai, Y. Yu, Z. Jiang, Z. Chen, J. Chen, Z. Yu, J. Zhai, N. Zhang, L. Tian, F. Wu, G. Yang, Z.-C. Hao, and J. Y. Zhou, "The Role of Millimeter-Wave Technologies in 5G/6G Wireless Communications," *IEEE Journal of Microwaves*, vol. 1, no. 1, pp. 101–122, 2021.